Proceedings of the Thirty Ninth National Conference on Fluid Mechanics and Fluid Power

December 13-15, 2012, SVNIT Surat, Gujarat, India

FMFP2012 - 135

NUMERICAL STUDY OF AXIAL BACK CONDUCTION IN MICROTUBES

Manoj Kumar Moharana
Assistant Professor
Department of Mechanical Engineering
National Institute of Technology Rourkela
Rourkela-769008, Odisha, India
e-mail: moharanam@nitrkl.ac.in

Sameer Khandekar
Associate Professor
Department of Mechanical Engineering
Indian Institute of Technology Kanpur
Kanpur-208016, U.P, India
e-mail: samkhan@iitk.ac.in

ABSTRACT
A two dimensional numerical simulation is carried out to study the effect of axial wall conduction in a microtube in conjugate heat transfer situations. Both, constant wall heat flux and constant wall temperature, at the outer surface of the tube are analyzed while flow of fluid through the microtube is laminar, simultaneously developing in nature. The cross-sectional solid faces are considered adiabatic. A microtube of length 120 mm and internal radius 0.2 mm is considered while the thickness of the tube wall is varied. Simulations have been performed for a wide range of tube wall to convective fluid conductivity ratio ($k_{sf} \approx 0.33$ - 702), tube thickness to inner radius ratio ($\delta_{sf} \approx 1$, 16), and flow Reynolds number (Re ≈ 100, 1000). The results show that k_{sf} plays a dominant role in the conjugate heat transfer process. For constant heat flux applied on the outer surface of the microtube, there exists an optimum value of k_{sf} at which the average Nusselt number ($\overline{Nu}$) over the microtube length is maximum; it decreases with departure from this optimum k_{sf} value. However, for constant wall temperature on the outer surface of the microtube, no such optimum k_{sf} value is observed at which $\overline{Nu}$ is maximum. The value of $\overline{Nu}$ is found to be increasing with decreasing value of k_{sf}. Secondly, thicker wall leads to higher $\overline{Nu}$.

KEYWORDS
Conjugate heat transfer, Thermally developing flow, Axial back conduction, Optimum Nusselt number, Constant heat flux and constant temperature boundary conditions.

INTRODUCTION
In recent times there has been an increasing trend towards miniaturization of appliances. As a result, microtubes are frequently being used for a variety of engineering applications. The ratio of the thickness of the tube wall to the inner radius in microtubes is very high, unlike a conventional tube where this ratio is very small. This is due to microscale inner tube diameter, along with the physical necessity of certain minimum thickness of the tube wall, which otherwise cannot be proportionately reduced due to ease in handling during and after production. The relative thickness of the solid wall of a microtube compared to its inner radius leads to multi-dimensional conjugate heat transfer, depending on several other factors, viz., thermo-physical properties of the solid substrate and fluid involved, and flow conditions.

Unlike a conventional system, negligence of axial heat conduction along the solid walls of micro heat exchangers frequently leads to erroneous conclusions and inconsistencies in the interpretation of transport data. Nevertheless, in actual practice, the temperature and heat flux distribution at the

conjugate wall(s) of the channel(s) depends on many factors, such as dimensions of both the solid and the fluid domain, thermal properties of solid/fluid involved, and flow characteristics of working fluid, etc. In reality, the boundary condition(s) is (are) applied at a certain finite distance from the actual solid-fluid interface, whereas the objective ought to be the maintenance of constant heat flux at the solid-fluid interface for maximizing the heat transfer coefficient or maintaining constant wall temperature for some specific applications.

LITERATURE REVIEW

The study of axial back conduction in the solid domain in a convective heat transport system dates back to the era of sixties when Bahnke and Howard, 1964, studied the effect of longitudinal heat conduction on the performance of periodic-flow heat exchanger. Soon afterwards, Petukhov, 1967, studied the effect of thermal conductivity ratio of the solid walls and the working fluid, and the tube thickness to inner radius ratio on the axial back conduction in the solid wall of a circular tube. Subsequently, some similar studies were carried out by many researchers (Chiou, 1980; Faghri and Sparrow, 1980; Cotton and Jackson, 1985). The study on axial conduction continued with time, but their number was very few. Subsequently, with the development of microscale heat transfer devices the study on axial conduction has again gained momentum, considering the relative importance of axial conduction effect in such small geometries, as compared to conventional sized heat transfer devices. Peterson, 1999, numerically studied conduction effects in microscale counter flow heat exchangers. Maranzana et al., 2004, introduced axial conduction number (M), defined as the ratio of the conductive heat flux to the convective counterpart. Maranzana et al., 2004, also stated that axial conduction in the solid substrate will be negligible if $M < 0.01$. Based on their study on conjugate heat transfer in thick circular tubes Li et al., 2007, and Zhang et al., 2010, concluded that the criteria proposed by Maranzana et al., 2004, for neglecting axial conduction may not be always valid in certain cases. Depending on the boundary conditions and geometrical parameters, the criteria for judging the effect of axial wall conduction may vary depending on the situation.

Recently, Moharana et al. 2012, carried out numerical analysis of axial conduction in a circular micro tube and a square shaped microchannel on a solid substrate. Both the circular microtube and the square microchannel are subjected to constant wall heat flux. Their study, based on wide parametric variations, suggests that for both the microtube as well as square microchannel on a solid substrate, there exists an optimum value of conductivity ratio (conductivity of the solid substrate material to conductivity of working fluid) which maximizes the average Nusselt number over the channel length (for constant heat flux boundary condition applied at the outer walls of the tube/channel). This observation was based on an extensive parametric variation of conductivity ratio, flow Re and substrate thickness, while the heating perimeter was kept constant, i.e., a square channel of constant dimensions and a microtube of constant inner diameter. This can be explained as follows for the square microchannel: Higher conductivity ratio leads to severe axial back conduction, thus decreases average Nu. Very low value of conductivity ratio leads to a situation which is qualitatively similar to the case of zero thickness substrate with constant heat flux applied on one wall only (the other three sides being adiabatic). This again lowers the average value of Nusselt number.

Although a number of theoretical (Hetsroni et al., 2005), experimental (Celata et al., 2006; Hetsroni et al., 2005; Li et al., 2007; Liu et al., 2007; Liu et al., 2011), and numerical (Li et al., 2007; Avci et al., 2012) studies have been performed, discerning parameters for explicitly isolating the effect of axial conduction on transport coefficient are not available. In this background, a two-dimensional numerical investigation is carried out on using commercial Ansys-Fluent® platform, to understand and highlight the effect of tube thickness to inner radius ratio (δ_{sf}), solid wall to working fluid conductivity ratio (k_{sf}) and flow Re on the axial wall conduction in a steady-state laminar, incompressible, simultaneously developing flow in microtubes. Both, uniform wall heat flux and uniform wall temperature boundary condition is considered, applied at the outer surface of the tube, so as to find out the effect of these conditions on the axial conduction in the microtube and hence on the ensuing heat transfer.

The cross-sectional solid faces are considered adiabatic. Thermophysical properties of the solid and the fluid domain are assumed to be constant. Local wall heat flux, wall temperature and average bulk fluid temperature are numerically calculated as functions of the dimensionless axial distance (x/L), thickness to inner radius ratio (δ_{sf}), and conductivity ratio (k_{sf}). Simulations have been carried out for a wide range of k_{sf} (≈ 0.33 - 702) and δ_{sf} = 1, 16, Re = 100, 1000. These parametric variations cover the typical range of applications encountered in micro-fluids/micro-scale heat transfer domains. Wall heat flux, wall temperature and average bulk fluid temperature along the length of the microtube are numerically calculated as functions of the variable parameters. Grid independence was also ensured before deciding the grid size in all the geometries.

NUMERICAL ANALYSIS

In this work it is assumed that the flow through the microtube is laminar, incompressible with constant thermo-physical properties, the heat transfer and fluid flow takes place at steady state, and the amount of heat loss by radiation or natural convection is negligible. Figure 1. shows a microtube of inner radius δ_f, thickness δ_s, and of length L. The value of inner radius δ_f, and the length L are kept constant in the computational model at 0.2 mm, and 120 mm respectively. The thickness of the microtube is varied (δ_{sf} = 1.0, 16.0).

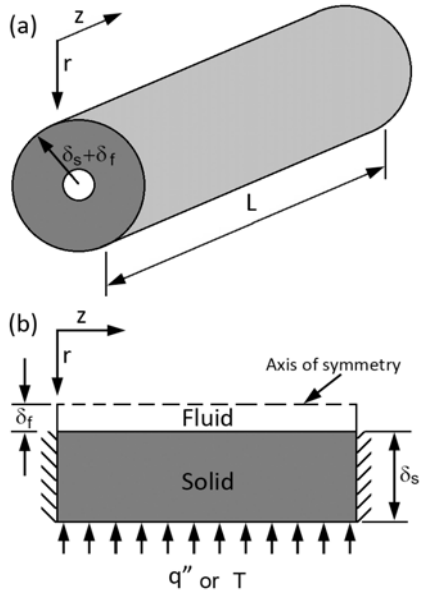

Figure 1: Microtube and its computational domain

In actual computations, two-dimensional Cartesian coordinate system (here named as r-z) with axisymmetric about the tube axis is considered. As discussed earlier, a constant heat flux as well as constant wall temperature boundary condition is respectively applied on the outer surface of the tube and the cross-sectional solid faces are insulated, as shown in Fig. 1.

The continuity, Navier-Stokes, and energy equations are as follows:

Liquid domain:

$$\nabla \cdot \vec{u} = 0 \tag{1}$$

$$\vec{u} \cdot \nabla \vec{u} = -\frac{1}{\rho}\nabla p + \frac{\mu}{\rho}\nabla^2 \vec{u} \tag{2}$$

$$\vec{u} \cdot \nabla T = \frac{k}{\rho C_p}\nabla^2 T \tag{3}$$

Solid domain:

$$\nabla^2 T = 0 \tag{4}$$

The associated boundary conditions are as follows:

$$\frac{\partial T}{\partial z} = 0 \text{ at } z = 0, L \text{ and } \delta_f \le r \le (\delta_f + \delta_s) \tag{5a}$$

$$q'' = 0 \text{ or } T = \text{constant at } r = \delta_f + \delta_s \tag{5b}$$

$$-k\frac{\partial T}{\partial r} = h(T - T_f) \text{ at } r = \delta_f \tag{5c}$$

$$u = \bar{u} \text{ at } z = 0 \tag{5d}$$

$$u = 0 \text{ at } r = \delta_f \tag{5e}$$

$$p = 0 \text{ at } z = L \tag{5f}$$

$$\frac{\partial T}{\partial r} = 0, \ \frac{\partial u}{\partial r} = 0 \text{ at } r = 0 \tag{5g}$$

Above equations are solved using commercial platform Ansys-Fluent®. For pressure discretization the 'standard' scheme was used. The SIMPLE algorithm was used for velocity-pressure coupling in the multi-grid solution procedure. The momentum and energy equations were solved using 'second-order upwind'. An absolute convergence criterion for continuity and momentum equations is taken as 10^{-6} and for energy equation it is 10^{-9}. Water is used as the working fluid; it enters the microtube with a slug velocity profile, at an inlet temperature of 300K. Thus, the flow is hydrodynamically as well as thermally developing in nature at the tube inlet.

The computational domain was meshed using rectangular elements and the grid independence test

was carried out before finalizing the grid size. As an example, local Nusselt number, calculated for a microtube with δ_{sf} = 0 (zero wall thickness), for three mesh sizes of 8×960, 10×1200 and 12×1440 (for half of the transverse section as shown in Fig. 1b.), for Re = 250, is as shown in Fig. 2. The local Nusselt number at the fully developed flow regime (near the tube outlet) changed by 0.2% from the mesh size of 8×960 to 10×1200, and changed by less than 0.1% on further refinement to mesh size of 12×1440.

Moving from first to the third mesh, no appreciable change is observed. So, the intermediate grid (10×1200) was selected, which corresponds to actual physical average spacing of 0.02 mm along the radial direction and 0.1 mm along the transverse direction (z-axis). It can also be observed in Fig. 2. that the local Nusselt number values in the fully developed region coincides with Nu_T = 3.66 where Nu_T is the Nusselt number for fully developed flow in a tube subjected to constant wall temperature. Finer meshing was used at the tube entrance and at the boundary layer.

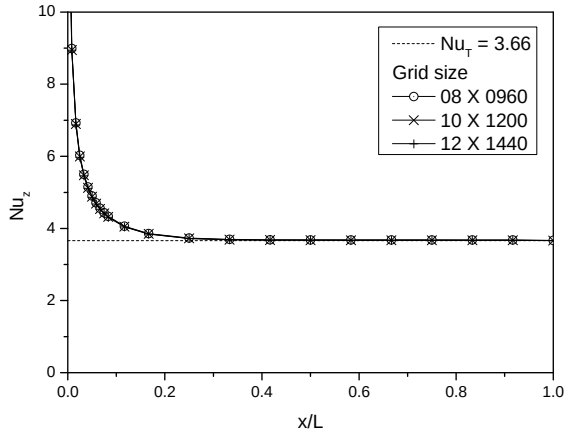

Figure 2: Variation of local Nusselt number calculated along the streamwise direction of a microtube of length 120 mm and δ_{sf} = 0 for three different mesh sizes.

DATA REDUCTION

The main parameters of interest are (a) local heat flux (b) local bulk fluid temperature (c) local wall temperature. These parameters allow us to determine the extent of axial conduction on the local Nusselt number. The conductivity ratio (k_{sf}) is defined as the ratio of thermal conductivity of the tube wall (k_s) to that of the working fluid (k_f). The axial coordinate, z, in dimensionalized as:

$$z^* = \frac{z}{L} \tag{6}$$

For constant heat flux boundary condition, the heat flux applied on the outer surface of the tube is:

$$\overline{q''_o} = \frac{Q}{2 \cdot \pi \cdot (\delta_s + \delta_f) \cdot L} \tag{7}$$

where, Q is the total heat input to the outer surface of the tube. The ideal heat flux at the solid fluid interface is given by:

$$\overline{q''} = \overline{q''_o} \frac{(\delta_s + \delta_f)}{\delta_f} \tag{8}$$

The non-dimensional local heat flux at the fluid-solid interface is given by:

$$\phi = q''_z / \overline{q''} \tag{9}$$

where, q''_z is the local heat flux transferred at the solid-fluid interface along the tube length. The dimensionless bulk fluid and tube inner wall temperatures are given by:

$$\Theta_f = \frac{\overline{T}_f - \overline{T}_{fi}}{\overline{T}_{fo} - \overline{T}_{fi}} \tag{10}$$

$$\Theta_w = \frac{\overline{T}_w - \overline{T}_{fi}}{\overline{T}_{fo} - \overline{T}_{fi}} \tag{11}$$

where, $\overline{T}_{fi}$ and $\overline{T}_{fo}$ are the average bulk fluid temperature at the tube inlet and outlet respectively; $\overline{T}_f$ is the average bulk fluid temperature at any location and $\overline{T}_w$ is the wall temperature at the same location. The local Nusselt number is then given by:

$$Nu_z = h_z \cdot D / k_f \tag{12}$$

where, the local heat transfer coefficient is:

$$h_z = \frac{q''_w}{\overline{T}_w - \overline{T}_f} \tag{13}$$

RESULTS AND DISCUSSION

Under ideal conditions (zero wall thickness and constant wall temperature), the non-dimensional fluid temperature must asymptotically approach the wall temperature with a negative exponent as it flows through the tube in the streamwise direction. In contrast, under ideal conditions (zero wall thickness and constant heat flux boundary condition), the non-dimensional fluid temperature

increases linearly in the entire flow domain (developing as well as fully developed). In this case however, the wall temperature increases non-linearly in the developing region while for fully developed region, it follows a linear increase. Hence, the difference between the wall and bulk fluid temperature is a constant in the fully developed region.

In this background, the case of constant wall temperature on the outer surface of the tube is considered first and axial variation of dimensionless average bulk fluid and tube inner wall temperature are shown in Fig. 3. For the case when flow Re = 100, k_{sf} = 702 (Fig. 3a), the system nearly follows the ideal behaviour (for both δ_{sf}). However, keeping the flow Re same and reducing the k_{sf} to 0.33 (Fig. 3b) drastically changes the variation of both the wall as well as the bulk fluid temperature. The wall temperature is no more constant at the fluid solid interface. Also, the fluid temperature now changes and tends towards a linear variation (dotted line included for comparison). In this case, increasing δ_{sf} from 1 to 16 also has a profound effect of the axial variation of both temperatures; they drift further away from ideal behaviour with increasing tube thickness.

In Figs. 3c and 3d, the flow Re is increased to 1000, and k_{sf} are changed to 702 and 0.33, respectively. In Fig. 3c. it can be observed that the wall temperature is almost constant except near the inlet, and the variation of fluid temperature is quite different from ideal, tending to be closer to 'linear'. In addition, the results are independent of δ_{sf}. With increasing Re and decreasing k_{sf}, the most dramatic change in the system behaviour is observed. The trends for axial variation of wall and fluid now come closer to the 'ideal' case of constant heat flux condition, rather than constant wall temperature condition. Thus, the constant temperature boundary condition imposed at a distance from the actual fluid-solid interface manifests itself as if the actual fluid-solid interface was supplied with a constant heat flux boundary condition. Thus, increasing Re and decreasing k_{sf} leads to a situation very similar to the case of a tube subjected to constant heat flux boundary condition. It is therefore expected that this situation will lead to higher Nusselt number among all other combinations reported here.

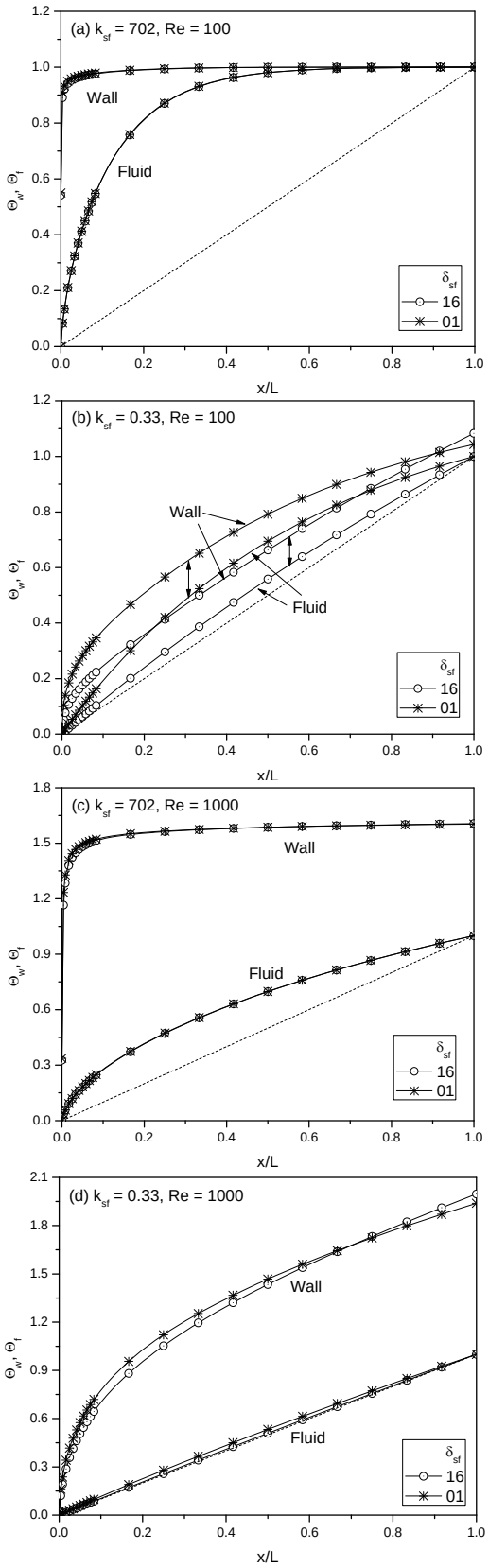

Figure 3: Variation of dimensionless local wall and local bulk fluid temperature along the channel length.

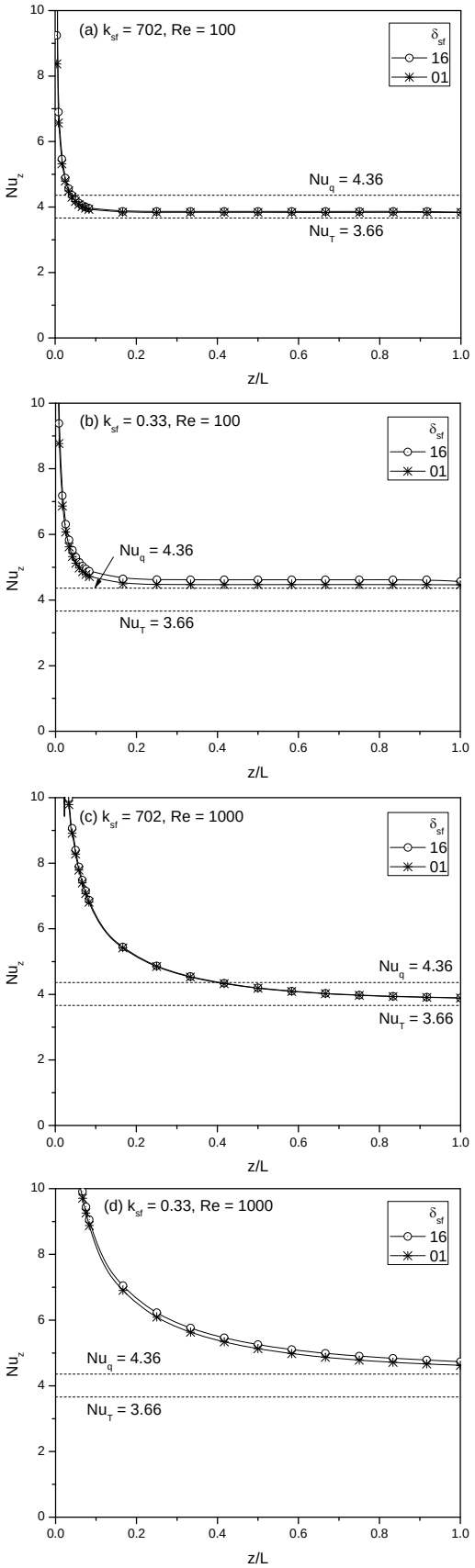

Figure 4: Variation of local Nusselt Number along the channel length.

In addition to the above, it can also be concluded from the general trends of Fig. 3 that the thickness of the tube (i.e. δ_{sf}) plays a role at lower flow Re only; with increasing flow Re the effect of δ_{sf} diminishes. Secondly, the effect of δ_{sf} further becomes negligible with higher k_{sf}. The contents in Fig. 3. represent higher and lower limits of k_{sf}, Re and δ_{sf} values considered in this study.

The direct implication of the axial variation of wall and bulk fluid temperature, as outlined in Fig. 3., decides the value of local Nusselt number, as presented next in Fig. 4. For benchmarking, the fully developed Nusselt number values for constant wall heat flux (Nu_q = 4.36) and constant wall temperature (Nu_T = 3.66) are also depicted. As expected, the fully developed Nusselt number values for k_{sf} = 702 and Re = 100 (corresponding to Fig. 3a), as depicted in Fig. 4a. is closer to the 'ideal' case of Nu_T. In contrast, for k_{sf} = 0.33 and Re = 1000 (corresponding to Fig. 3d), it is clear that the local Nusselt number will eventually be higher, closer to ideal case of constant heat flux boundary condition, Nu_q. It is clear from this discussion that boundary condition, as experienced by the fluid can be drastically altered by axial conduction coupled with the developing nature of the flow.

To understand the explicit effect of k_{sf} on heat transfer more clearly, the variation of average Nusselt number ($\overline{Nu}$) over the length of the tube, as a function of k_{sf}, while varying flow Re and δ_{sf}, is presented in Fig. 5a., where constant wall temperature condition is applied on the tube outer surface. It can be seen that for fixed value of Re and δ_{sf}, the value of $\overline{Nu}$ increases, as the value of k_{sf} decreases. The slope of this curve changes rapidly below k_{sf} less than 100 and the value of $\overline{Nu}$ increases sharply, as the value of k_{sf} approach towards zero, suggesting that lower k_{sf} results in higher $\overline{Nu}$. With increasing flow Re at constant k_{sf}, the $\overline{Nu}$ value increases due to increase in flow development length. Secondly, it can also be observed that for all other parameters remaining the same, higher wall thickness leads to higher value of $\overline{Nu}$. Finally, the gap between the curves at δ_{sf} = 1 and 16 increases with decreasing value of k_{sf}.

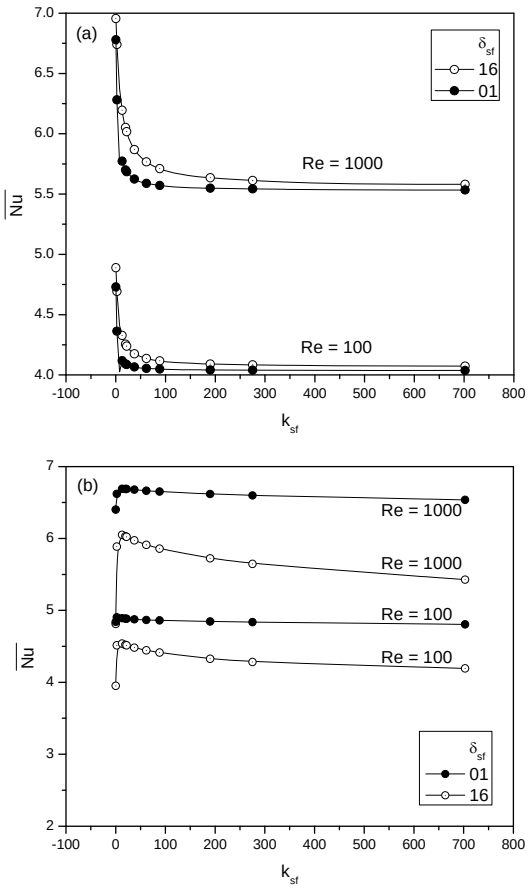

Figure 5: Variation of $\overline{Nu}$ as a function of k_{sf} for a microtube subjected to boundary condition of (a) constant wall temperature (b) constant heat flux at its outer surface.

Figure 5b. depicts the corresponding plot for constant wall heat flux applied on the outer surface of the microtube. For this case, the presence of optimum k_{sf} at which the average Nusselt number is maximum, can be observed clearly. Secondly, all other parameters remaining constant, the average Nusselt number decreases as the value of δ_{sf} increases from 1 to 16. This is exactly opposite to that of Fig. 5a. This is because axial conduction in a microtube subjected to constant heat flux at the outer surface drifts the condition at the inner surface of the tube towards a conventional constant wall temperature boundary condition. On the other hand, axial conduction in a microtube subjected to constant wall temperature at the outer surface drift the condition at the inner surface of the tube towards a conventional constant heat flux boundary condition.

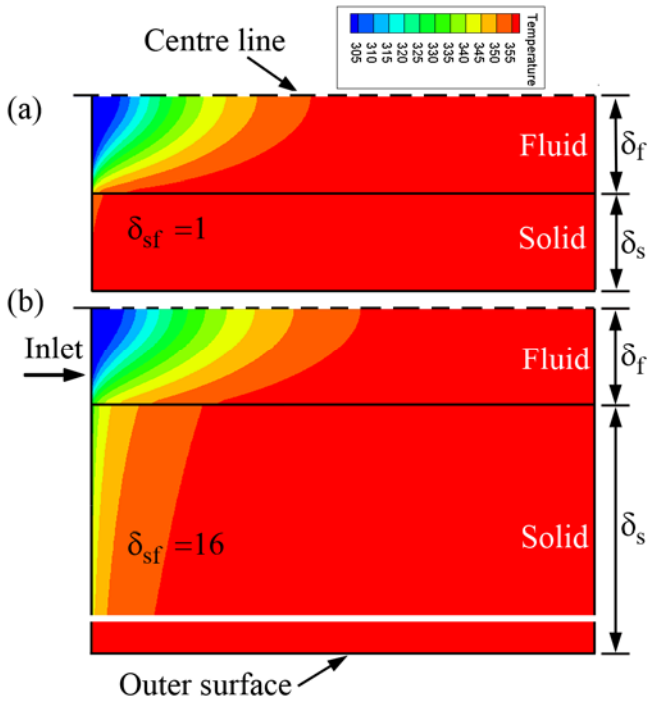

Figure 6: Temperature contour in the solid and the fluid domain along the transverse plane of a microduct subjected to constant wall temperature T = 360 K at Re =100, k_{sf} = 12.8 and (a) δ_{sf} = 1.0, (b) δ_{sf} = 16.

Figure 6a and 6b shows the temperature contour in the solid and the fluid domain along the transverse plane of a microduct subjected to constant wall temperature T = 360 K at Re =100, k_{sf} = 12.8 for two geometries of δ_{sf} = 1.0 and 16 respectively. The solid fluid interface is represented by the horizontal line between the solid and the fluid domain. For δ_{sf} = 1.0, the temperature at the solid-fluid interface is uniform throughout the length of the microduct and equal to the applied value at the outer surface (top face in Fig 6). This can be observed in Fig. 6a. However, for δ_{sf} = 16, this is not true. Due to higher wall thickness compared to inner radius, the axial back conduction causes deviation from uniform wall temperature at the solid-fluid interface. It can be seen in Fig. 3b, for similar conditions, the axial variation of wall temperature at the solid-fluid interface drifts more towards the trend of constant heat flux rather than constant wall temperature. This causes higher Nusselt number compared to thinner tube wall thickness, which can also be observed in Fig. 5a for Re =100, k_{sf} = 12.8 and δ_{sf} = 1.0, and 16.

SUMMARY AND CONCLUSIONS

A two dimensional axisymmetric numerical investigation is carried out for flow through a microtube of length 120 mm and inner radius 0.2 mm. Varying tube wall thickness ($\delta_{sf} \sim 1, 16$), tube material ($k_{sf} \sim 0.33$ - 702) and flow condition ($Re \sim 100, 1000$) is used to find their effect on axial back conduction in the solid wall of the tube. Flow is simultaneously developing in nature.

It is shown that a constant temperature boundary condition applied on the outer surface of the tube can manifest itself as a constant heat flux boundary condition on the actual fluid-solid interface, depending on the control parameters, i.e. k_{sf}, Re, and δ_{sf}. The thermal conductivity ratio plays the most important role.

For constant heat flux boundary condition on the outer surface of the tube, it is found that there exists an optimum conductivity ratio (k_{sf}) at which $\overline{Nu}$ over the microtube length maximizes. However, no such maxima in $\overline{Nu}$ is observed corresponding to any value of conductivity ratio for constant wall temperature boundary condition. For this case (i) $\overline{Nu}$ decreases with increasing k_{sf} and, (ii) thicker wall leads to higher value of $\overline{Nu}$.

ACKNOWLEDGMENTS

The work is funded by the Department of Science and Technology, Government of India, under the sponsored project No: DST/CHE/20060304 titled 'Micro-devices for Process Applications'.

NOMENCLATURE

C_p specific heat of working fluid, J/kg-K
D diameter (inner) of the tube, m
h_z local heat transfer coefficient, W/m^2-k
k_f thermal conductivity of working fluid, W/m-K
k_s thermal conductivity of tube wall, W/m-K
k_{sf} ratio of k_s and k_f (-)
L length of the tube, m
Nu_z local Nusselt number ($h_z D/k_f$)
$\overline{Nu}$ average Nusselt number over the channel length
Pr Prandtl number ($C_p\mu/k_f$)
Q applied heat on outer surface of the tube, W
$\overline{q''}$ average heat flux experienced at the inner surface of the tube, W/m^2
$\overline{q''_o}$ applied heat flux on tube outer surface, W/m^2
Re Reynolds number ($\rho uD/\mu$)
T temperature, K
$\overline{T}$ average temperature, K
u average fluid velocity at the tube inlet, m/s
z axial coordinate
z* non-dimensional axial distance along the microtube (-)

Greek symbols

δ_f inner radius of the tube, m
δ_s thickness of the tube wall, m
δ_{sf} ratio of δ_s and δ_f (-)
μ dynamic viscosity, Pa-s
ρ density, kg/m^3
ϕ non-dimensional local heat flux (-)
Θ non-dimensional temperature (-)

Subscripts

f fluid
i inlet condition
o outlet condition
q refers to the case of constant heat flux boundary condition
s solid
T refers to the case of a constant wall temperature boundary condition
w wall surface
z axial length along the channel

REFERENCES

Avci, M., Aydin, O., Arici, M.E., 2012. Conjugate heat transfer with viscous dissipation in a microtube, International Journal of Heat and Mass Transfer 55 (19-20) 5302-5308.

Bahnke, G.D., Howard, C.P., 1964. The effect of longitudinal heat conduction on periodic-flow heat exchanger performance, Journal of Engineering Power 86 (1) 105-120.

Celata, G.P., Cumo, M., Marconi, V., McPhail, S.J., Zummo, G., 2006. Microtube liquid single-phase heat transfer in laminar flow, International Journal of Heat and Mass Transfer 49 (19-20) 3538-3546.

Chiou, J.P., 1980. The advancement of compact heat exchanger theory considering the effects of longitudinal heat conduction and flow non-uniformity. symposium on compact heat exchangers-history, technological advancement and mechanical design problems. Book no. G00183, HTD Vol. 10, ASME, New York.

Cotton, M.A., Jackson, J.D., 1985. The effect of heat conduction in a tube wall upon forced convection heat transfer in the thermal entry region, In: Numerical methods in thermal problems, vol. (iv), Pineridge Press, Swansea, 504-515.

Faghri, M., Sparrow, E.M., 1980. Simultaneous wall and fluid axial conduction in laminar pipe-flow heat transfer, Journal of Heat Transfer 102 (1) 58-63.

Hetsroni, G., Mosyak, A., Pogrebnyak, E., Yarin, L.P., 2005. Heat transfer in micro-channels: Comparison of experiments with theory and numerical results, International Journal of Heat and Mass Transfer 48 (25-26) 5580-5601.

Li, Z., He, Y.L., Tang, G.H., Tao, W.Q., 2007. Experimental and numerical studies of liquid flow and heat transfer in microtubes, International Journal of Heat and Mass Transfer 50 (17-18) 3447-3460.

Liu, Z., Liang, S., Zhang, C., Guan, N., 2011. Viscous Heating for Laminar Liquid Flow in Microtubes, Journal of Thermal Science 20 (3) 268-275.

Liu, Z., Zhao, Y., Takei, M., 2007. Experimental study on axial wall heat conduction for convective heat transfer in stainless steel microtube, Heat Mass Transfer 43 (6) 587-594.

Maranzana, G., Perry, I., Maillet, D., 2004. Mini- and micro-channels: influence of axial conduction in the walls, International Journal of Heat and Mass Transfer 47 (17-18) 3993-4004.

Moharana, M.K., Khandekar, S., 2012. Optimum Nusselt number for simultaneously developing internal flow under conjugate conditions in a square microchannel, Journal of Heat Transfer 134 (7) 071703(01-10).

Peterson, R.B., 1999. Numerical modeling of conduction effects in microscale counter flow heat exchangers. Microscale Thermophysical Engineering 3 (1) 17-30.

Petukhov, B.S., 1967. Heat transfer and drag of laminar flow of liquid in pipes. Energiya, Moscow.

Türkakar, G., Okutucu-Özyurt, T., 2012. Dimensional optimization of microchannel heat sinks with multiple heat sources. International Journal of Thermal Sciences, (in press, DOI: 10.1016/j.ijthermalsci.2011.12.015).

Zhang, S.X., He, Y.L., Lauriat, G., Tao, W.Q., 2010. Numerical studies of simultaneously developing laminar flow and heat transfer in microtubes with thick wall and constant outside wall temperature, International Journal of Heat and Mass Transfer 53 (19-20) 3977-3989.